Numerical Simulation of Air Flow and Gas Dispersion around Obstacles

The-Duc Nguyen*1, Ngoc-Hai Duong*1, Warn-Gyu Park*2

Abstract

Computations of the mean and turbulence flows over three-dimensional hill of conical shape have implemented. Beside the standard $k-\epsilon$, two other modifications proposed by Detering & Etling and Duynkerke for atmospheric applications were also considered. These predictions were compared with the data of a wind tunnel experiment. From the comparison, it was concluded that all three models predict the mean flow velocities equally well while only the Duynkerke's model accurately predicts the turbulence data statistics. It also concluded that there are large discrepancies between model predictions and the measurements near the ground surface.

The flow field, which was obtained by using the Duynkerke's modification, was used to simulate gas dispersion from an upwind source. The calculation results are verified based on the measurement data. Modifications of the turbulent Schmidt number were carried out in order to match the measured results. The code was used to investigate the influence of the recirculation zone behind a building of cubical shape on the transport and dispersion of pollutant. For a stack behind and near the obstacle, some conclusions about the effect of the stack height and stack location were derive

1. Introduction

To simulate turbulent flow in the atmospheric boundary layer, the first-order closure model (K-theory) has been widely applied (see e.g. [1]-[6]). This model employs a diagnostic formula for the length scale or mixing length. However it is difficult to prescribe the mixing-length distribution in situations other than simple shear-layer flow, therefore, in reality, the first-order closure model is not applicable for describing flows with complex structure. The second and higher order closure models employ transport equations for the individual Reynolds stress and turbulent fluxes derived from the Navier-Stokes equations. Normally they contain terms explicitly taking into account the influence of buoyancy forces on the Reynolds stresses and turbulent fluxes [1]. However, the resulting model is quite complex, therefore less suitable for solving practical problems.

An intermediate one-and-haft order closure model, so-called, the k-εturbulence model [7] requires only two more additional prognostic equations in comparison with the first-order closure model. This model has been found to be a successful compromise between capability and simplicity.

The standard k-ε model [7] has been shown to work quite well for describing many different flows. It has been also applied to describe atmospheric flows from a simple atmospheric

*1. Institute of Mechanics, NCST of Vietnam. Email: dnhai@im01.ac.vn
*2. Pusan National University, Korea. Email: wgpark@pusan.ac.kr
Corresponding author Ngoc-Hai Duo

boundary layer to complex circulation flows, such as land-sea breeze and pollutant dispersion near an irregular terrain [8]-[10]. However, for modeling atmospheric turbulence flows, some authors recommended a number of modifications of the standard k-ε model ([12], [13]).

The objective of this study is also related to the application of k-ε model for three-dimensional simulation of wind field and pollutant dispersion. Computations of the mean and turbulence flows over three-dimensional hill of conical shape have implemented. Beside the standard k-ε , two other modifications proposed by Detering & Etling and Duynkerke for atmospheric applications were also considered. These predictions were compared with the data of a wind tunnel experiment. The flow field, which was obtained by using the Duynkerke's modification, was used to simulate gas dispersion from an upwind source. The calculation results are verified based on the measurement data. Modifications of the turbulent Schmidt number were carried out in order to match the measured results. The code was also used to investigate the influence of the recirculation zone behind a building of cubical shape on the transport and dispersion of pollutant.

2. Description of theoretical models

The Reynolds-averaged Navier-Stockes equations governing the motion of turbulent flows and pollutant dispersion may be written in the Cartesian coordinates as

$$\frac{\partial(\rho U_i)}{\partial x_i} = 0 \tag{1}$$

$$\frac{\partial U_i}{\partial t} + U_j\frac{\partial U_i}{\partial Ux_j} = -\frac{\partial(\overline{u_i'u_j'})}{\partial x_j} - \frac{1}{\rho_0}\frac{\partial \delta P}{\partial x_i} + \frac{\delta\rho}{\rho_0}g_i \tag{2}$$

$$\frac{\partial \Theta}{\partial t} + U_j\frac{\partial \Theta}{\partial x_j} = -\frac{\partial(\overline{\theta' u_j'})}{\partial x_j} \tag{3}$$

$$\frac{\partial C}{\partial t} + U_i\frac{\partial C}{\partial x_i} = -\frac{\partial(\overline{u_i'c'})}{\partial x_i} + S \tag{4}$$

where: U_i Θ, and C are the mean components of the velocity, potential temperature and concentration, respectively; u_i', θ' and c' are the fluctuations of the velocity components, potential temperature and concentration, respectively; $g_i = (0,0,-g)$ are the components of the gravitational acceleration, $\delta\rho$ is the deviation of density ρ from its reference value ρ_0, δP is the deviation of pressure P from its reference P_0, and S is the mass generation rate. The subscript 0 refers to the aerostatic and adiabatic reference state [14].

The pressure is related to the density and the temperature T through the following equation of state:

$$P = \rho R_d T \tag{5}$$

The potential temperature is defined as $\Theta = T(P/P_a)^{\frac{R}{C_p}}$ where P_a is the surface pressure at $z=0$, R_d is the gas constant for dry air $(R_d = 287\,Jkg^{-1}K^{-1})$ and C_p is the specific heat at constant pressure for air.

The Reynold stresses $\overline{u_i'u_j'}$, the turbulent heat flux $\overline{u_i'\theta'}$ and the turbulent concentration flux $\overline{u_jc'}$ are estimated by means of the Boussinesq's eddy viscosity and eddy diffusivity models ([15], [16]):

$$\overline{u_i'u_j'} = -\nu_t\left(\frac{\partial U_i}{\partial x_j}+\frac{\partial U_j}{\partial x_i}\right)+\frac{2}{3}\delta_{ij}k\ ;$$

$$\overline{u_i'\theta'} = -K_t\frac{\partial \Theta}{\partial x_i};$$

$$\overline{u_i'c'} = -K_c\frac{\partial C}{\partial x_i} \tag{6}$$

where is the eddy viscosity, is the Kronecker delta, is turbulent diffusivity coefficient and is turbulent diffusivity coefficient. The models assumes

$$\nu_t = c_\mu\frac{k^2}{\epsilon}\ ;\ K_t = \frac{\nu_t}{\mathrm{Pr}_t};\ K_c = \frac{\nu_t}{Sc_t} \tag{7}$$

where , and are empirical constants.

The turbulent kinetic energy and its dissipation rate are calculated from the following semi-empirical transport equations

$$\frac{\partial k}{\partial t}+U_j\frac{\partial k}{\partial x_j} = \frac{\partial}{\partial x_j}\left(\frac{\nu_t}{\sigma_k}\frac{\partial k}{\partial x_j}\right)+S+G-\epsilon \tag{8}$$

$$\frac{\partial \epsilon}{\partial t}+U_j\frac{\partial \epsilon}{\partial x_j} = \frac{\partial}{\partial x_j}\left(\frac{\nu_t}{\sigma_\epsilon}\frac{\partial \epsilon}{\partial x_j}\right) + \frac{\epsilon}{k}\left(c_{1\epsilon}S+c_{3\epsilon}G-c_{2\epsilon}\epsilon\right) \tag{9}$$

where $\sigma_k, \sigma_\epsilon, c_{1\epsilon}, c_{2\epsilon}$ and $c_{3\epsilon}$ are constants, S is the shear production term G and is the buoyancy term, defined as

$$S = \nu_t\left(\frac{\partial U_i}{\partial x_j}+\frac{\partial U_j}{\partial x_i}\right)\frac{\partial U_i}{\partial x_j}$$

and $$G = \frac{\nu_t}{\sigma_t}\frac{g}{\rho_0}\frac{\partial \rho}{\partial z}$$

In the above equations, the following standard values of the constants, which have been used for most engineering applications are given in Table 1. However, in the atmospheric turbulence modeling, some authors recommended making some change to the standard $k-\epsilon$ model on the basis of atmospheric data. Detering and Etling [12] proposed replacing the $c_{1\epsilon}$ and $c_{3\epsilon}$the constants by a function $c'_{1\epsilon}$ of dominant turbulent eddies L and the atmospheric boundary layer h

$$c'_{1\epsilon} = \frac{c_{1\epsilon}L}{h};L = \frac{c_\mu^{\frac{3}{4}}k^{\frac{3}{2}}}{\epsilon};h = c_h\frac{u_*}{f} \tag{10}$$

where $u_*$is the friction velocity, f is the Coriolis parameter, and c_h is an empirical constant, which was set by Detering and Etling to an optimum value of 0.0015.

In Duynkerke's modification [13], the contribution of the buoyancy in equation (9) is neglected when the term is negative. The other modifications of Detering & Etling and Duynkerke model are given in Table 1.

Table.1: Constants used in the conventional turbulence models

Turbulence model	c_μ	$c_{1\epsilon}$	$c_{2\epsilon}$	$c_{3\epsilon}$	σ_k	σ_ϵ
Standard	0.09	1.44	1.92	1.44	1.0	1.3
Detering and Etling [12]	0.026	*	1.90	*	0.74	1.3
Dunykerke [13]	0.033	1.46	1.90	1.46	1.0	2.38

*: See equations (10)

3. Solution procedure

For the flow fields, our numerical code is based on the SIMPLE method [21]. A finite volume method is applied on a staggered grid.

Because the equations for k and ϵ are much stiffer than the flow equations [22]. For this reason, in the numerical solution procedure, one first performs an outer iteration of the momentum

and pressure correction equations in which the value of the eddy viscosity is base on the values of k and ϵ at the end of the preceding iteration. After this has been completed, an outer iteration of the turbulent kinetic energy and dissipation equations is made. After completing an iteration of the turbulence model equations, we are ready to recalculate the eddy viscosity and start a new outer iteration.

4. Flow field simulation

The experiment of von-Karman Institute (VKI) was described in [23]. Measurements of the boundary layer (mean velocity and streamwise fluctuation velocity) and the flow structure over the conical hill were made using a hot-wide anemometer. This same flow was simulated using theoretical models. At the inflow boundary, variables are kept constant in time. Outflow conditions were those of well-developed flow; i.e. zero longitudinal gradients. A rigid lid is assumed at the upper boundary $z = z_{max}$ with zero normal velocity and zero normal gradients for other variables. Similar boundary conditions were assumed on y_{max} and y_{min}.

The boundary conditions at the lower boundary was determined by the standard wall-function treatment, implemented through an effective wall eddy viscosity. The details of this treatment are described by Ferziger and Perie [22].

Fig. 1 and Fig. 2 shows the velocity profiles at two locations and compare the computed results of three models with the wind tunnel simulation.

As shown in Fig. 1 and Fig. 2: the simulation results obtained using three models generally agree well with the measurements. It was difficult to tell the difference between standard and Duynkerke's models. Near the top of the model domain, it also was difficult to tell the difference about the simulation results of three models.

In this study, we estimated the streamwise velocity fluctuation u' from the turbulent kinetic energy k by using the definition of turbulent kinetic energy and with the following assumption:

$$k^2(x,y,z) = u'^2(x,y,z).f(z)$$

where $f(z)$ was calculated from profiles given by Robins and Castro [24]. In Fig. 3 and Fig. 4, the vertical profiles of the streamwise velocity fluctuation obtained from the simulations are compared with the corresponding measurements.

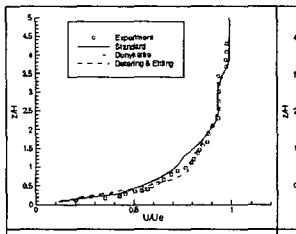

Fig.1: Mean velocity profilesfor experimental and simulated results at $x = -H$ and $y = 0$

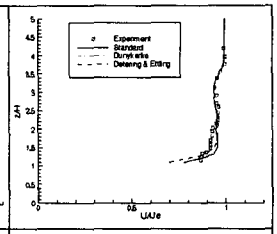

Fig.2: Mean velocity profiles for experimental and simulated results at $x = -H$ and $y = 0$ (over the crest of the hill).

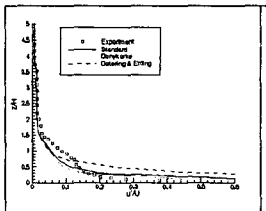

Fig. 3: Streamwise velocity fluctuation for experimental and simulated results at $x = -H$ and $y = 0$.

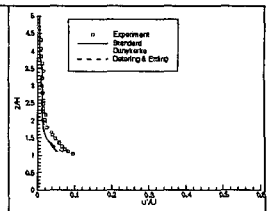

Fig. 4: Streamwise velocity fluctuation for experimental and simulated results at $x = 0$ and $y = 0$ (over the crest of the hill).

In general, the simulation results for velocity fluctuation do not agree with the measurements as well as in the case for the mean velocity. In addition, the simulated turbulence structure is

sensitive to the turbulence closure models. Comparing with the experimental data for the velocity fluctuation, the simulation results from the $k-\epsilon$ model with Duynkerke's modifications exhibit better agreement. The large disagreement was found in the results obtained using the Deterring and Etling's models.

5. Concentration field Simulation

In addition to the measurements of the flow field (velocity vector), the pollutant concentration measurement was also made in the VKI experiments. The stack in this experimental model was located at a distance of $3.7H$ upstream from the center of the hill (H is the height of the hill) i.e. $x_s = -3.7H$ and $y_s = 0$. Two measurements of the concentration field were performed for the stack height $h_s = H/2$ and H. These measured and calculated concentrations were normalized as

$$\chi = CU_eH^2Q^{-1} \qquad (11)$$

where χ= Normalized concentration; C= Concentration; U_e= Free stream velocity (velocity of flow before its entrance into the towing tank); H= Hill height and Q = Rate of source (g/s).

Because the simulated flow and turbulence fields of Duynkerke's model agree with measurement better than two remainders, so this model was used to perform numerical simulations presented in this study.

Many numerical simulations were performed with different turbulent Schmidt number Sc_t . Results of this numerical simulation indicated that, the variation of eddy mass diffusivity coefficients has a strong influence on the concentration field. It also indicated that an isotropic eddy mass diffusivity (i.e. the Schmidt number is the same in three direction) couldn't produce a calculated results close with the measurements. It may be expected that reasonable non-isotropic (especially between horizontal and vertical directions) eddy mass diffusivity will make the calculated results better.

The experimental data in the case $h_s = H$were used for the calibration based on assumption of the difference of turbulent Schmidt number between horizontal and vertical directions. The closest agreement with the experiment data was found in the case of $Sc_{t,y} = 0.61$and$Sc_{t,z} = 0.83$ (see Fig. 5). A verification of obtained Schmidt numbers was performed for the case of $h_s = H/2$. Fixed the Schmidt number $Sc_{t,x} = Sc_{t,y} = 0.61$; $Sc_{t,z} = 0.83$, we have calculated the concentration and obtained result satisfied as shown in Fig. 6.

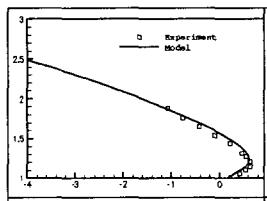

Fig. 5: Vertical concentration profiles above the crest of hill with $Sc_{t,x} = Sc_{t,y} = 0.61$; $Sc_{t,z} = 0.83$. $h_s = H/2$. z/H vs $log(x)$

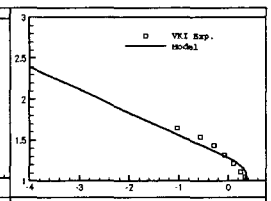

Fig. 6: Vertical concentration profiles above the crest of hill with $Sc_{t,x} = Sc_{t,y} = 0.61$; $Sc_{t,z} = 0.83$. $h_s = H/2$. z/H vs $\log x$

6. Effects of recirculation zone behind a building on ground-level concentration

The ground-level concentrations, which are defined as the concentration at the height of 1 m, are usually used to evaluate the atmospheric pollution because the concentrations at this level directly influence to humanity. Because of the important role of ground-level concentration, this study has performed several estimations of effects of the recirculation zone on the ground-level concentration when the stack must be set inside it.

Numerical experiments are performed for flow around a cubical building. The building height and widths are 60m. The approach flow is perpendicular to one of building's sides. The

following logarithmic wind law has been used for the approach flows:

$$\frac{u_0(z)}{u_{*0}} = \frac{1}{k}\ln\left(\frac{z-d}{z_0}\right) \qquad (12)$$

where: u_{*0} is the friction velocity; k is the von-Karman constant (~ 0.41); z_0 is the aerodynamic roughness length and d is the zero-plane displacement. The values of $u_{*0} = 0.15 m/s$ and $z_0 = 0.001 m$ are used in the flow field simulation using the $k-\epsilon$ model with the Duynkerke's modification. The velocity vectors in the vertical plane through the center of the building are shown in Fig. 7. In according to the calculation, the length of the recirculation zone behind building $L_R = 2.335H$.

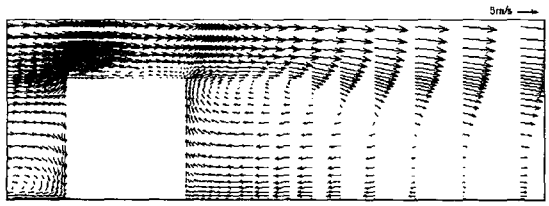

Fig. 7: Velocity vector field in the vertical plane through the center of building

The simulated flow field, which is described previously, is used to simulate concentration fields. The stack was set in the vertical plane through the center of building. The normalized concentration (11) is not dependent on the rate of source. The pollutants released are assumed passive. The concentration field simulation used a grid finer than the grid of flow field simulation. The numerical simulations were performed for stack located in different places near and behind the building. One of calculated results can be shown in Fig. 8. It is difficult to show all of result of these numerical experiments, therefore the mean ground-level concentration (in calculation domain) for each simulation were calculated and used as the indicator of the level of atmospheric pollution. The mean ground level concentration for different stack heights and stack locations are shown in Fig. 9.

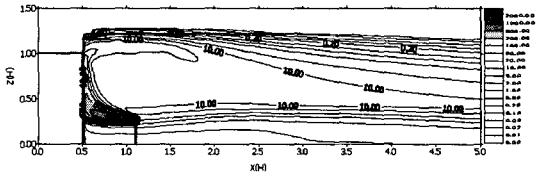

Fig. 8: Concentration contours in the vertical plane through the center of the building for the case of $x_s = 0.6H$ and $z_s = 0.3H$

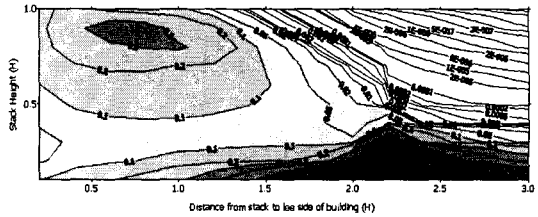

Fig. 9: Mean ground-level concentration contours as a function of stack height and stack location.

It was well known that, the higher stack would make the ground-level concentrations smaller. However, this tendency may be not true when the stack is set inside a recirculation zone. According to the calculated results of the ground-level concentration, we determined the best heights and the worst heights of a stack inside the recirculation zone when its distance to the building is fixed, which are shown in Fig. 10. It is noted that these best and worst heights are determined only in the condition that the stack does not exceed the obstacle height.

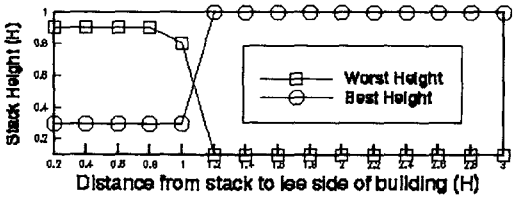

Fig. 10: The worst height and the best height as a function of the distance from the stack to the building

As show in Fig. 9, when the stack height is fixed because of some reasons, the location of the stack strongly influences to the concentration

fields at the ground surface level. From the calculated results of the ground-level concentration, we determined the best and the worst distance from the stack to the building as a function of the stack height, which are presented in Fig. 11.

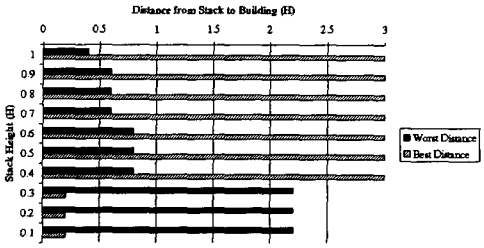

Fig. 11: The worst location and the best location of the stack as a function of the stack height.

7. Conclusions

Numerical simulations of turbulent flow over three-dimensional hill of conical shape [23] have been performed using a finite control volume method in a non-hydrostatic atmospheric model. Along with the standard $k-\epsilon$, two other modifications proposed by Detering & Etling and Duynkerke for atmospheric applications were also considered. From the comparison, it was concluded that all three models predict the mean flow velocities equally well while only the Duynkerke's model accurately predicts the turbulence data statistics. It also concluded that there are large discrepancies between model predictions and the measurements near the ground surface.

The calculated results of concentration fields indicated that the simulated concentration field is highly sensitive to the specification of eddy mass diffusivity and a non-isotropic dispersion model based on $k-\epsilon$ turbulence closure scheme with $Sc_{t,x} = Sc_{t,y} = 0.61$ and $Sc_{t,z} = 0.83$ gave the calculation results agree well with the experiment.

The existence of a building can cause the ground level concentration increase as many as several hundreds times. The effect of building on the ground level concentration of pollutants may be very weak when the stack height is greater than the building height about 1.2 times or when the distancefrom the stack to the building greater than the length of recirculation zone. It may very strong when the emission point locate near the center of main vortex or when the flow near the emission point is downward strongly.

Acknowledgement

This work was partly supported by the Natural Science Council of Vietnam. The paper is completed when Dr The-Duc Nguyen spent one year, during years of 2003 and 2004, to research under the supervisor of Professor Warn-Gyu Park, as a postdoctoral fellow of KOSEF at Pusan National Uni

References

[1] Garrat J.R., "The atmospheric boundary layer", Cambridge University Press, New York, (1992).

[2] Lyons T. J. and Scott W. D., "Principles of Air Pollution Meteorology", Belhaven Press, London, (1990).

[3] Physick W. L. et al., "LADM: A Lagrangian Atmospheric Dispersion Model", CSIRO Division of Atmospheric Research Technical Paper No.24, CSIRO, Australia, (1994).

[4] Duong Ngoc Hai, Nguyen The Duc, "Assess the predicted air quality impacts arising from operation of the proposed Quang Ninh Thermal Power Plant", Proceedings of the sixth National Conference of Mechanics, Hanoi, (1997).

[5] Duong Ngoc Hai, Nguyen Van Diep, Nguyen The Duc, Le Trinh, "Wind Field over Complex Terrain and Air Quality Modeling", J. Mechanics, NCNST of Vietnam, T.XIX, No 4, pp. 29-38, (1997).

[6] Jacbson M. Z., Lu R., Turco R. P. and Toon

O. B., "Development and Application of a new Air Pollution Modelling System Part I: Gas-Phase Simulation", Atmos. Environ., Vol. 30, No. 12, pp. 1939-1963, (1996).

[7] Rodi W. , "Turbulence Models for Environmental Problems". In Prediction Methods for Turbulent Flows, Ed. by Kollmann W., Hemisphere Publishing Corporation, Washington, 1980.

[8] Suttan S. B., Brandt H., and White B. R., "Atmospheric Dispersion of A Heavier-Than-Air Gas Near a Two-Dimensional Obstacle", Boundary-Layer Meteorol., Vol. 35, pp. 125-153, (1986).

[9] Mouzakis F. N. and Bergeles G., "Pollutant Dispersion Over a Triangular Ridge: A Numerical Study", Atmos. Environ., Vol. 25A, pp. 371-379, (1991).

[10] Stubley G. D. and Rooney D. R., "The sensitivity of $k-\varepsilon$ Model Computations of the Neutral Planetary Boundary Layer to Baroclinity", Boundary-Layer Meteorol., Vol. 37, pp. 53-70, (1986)..

[11] Riopelle G. and Stubley G. D., "The Influence of Atmospheric Stability on the "Leipzig" Boundary-Layer Structure", Boundary-Layer Meteorol., Vol. 46, pp. 207-227, (1989)..

[12] Detering H. W., and Etling D., "Application of the $E-\varepsilon$ turbulence model to the atmospheric boundary layer", Bound. Layer Meteor., Vol. 33, pp. 113-133, (1985).

[13] Duynkerke P. G., "Application of the $E-\varepsilon$ Turbulence Closure Model to the Neutral and Stable Atmospheric Boundary Layer", J. Atmos. Sci., Vol. 45, pp. 865-880, (1988).

[14] Clack T. L., "A Small-scale Dynamic Model Using a Terrain-Following Coordinate Transformation", J. Comp. Phys., Vol. 24, pp. 186-215, (1977).

[15] Mellor G. L. and Herring H. J. "A Survey of the Mean Turbulent Field Closure Models", AIAA Journal, Vol. 11, No. 5, pp. 591-599, (1973).

[16] Mellor G. L. and Yamada T., "A Hierarchy of Turbulence Closure Models for Planetary Boundary Layers. J. Atmos. Sci., Vol.31, pp. 1791-1806.

[17] Aspley D. D. and Castro I. P., "Numerical Modeling of Flow and Dispersion around Cinder Cone Butte", J. Atmos. Environ., 31(7), pp. 1059-1071, (1996).

[18] Sini J. F., Anquetin S. and Mestayer P. G., "Pollutant Dispersion and Thermal Effects in Urban Street Canyons", J. Atmos. Environ., 30(15), pp. 2659-2677, (1996).

[19] Kim J. J. and Baik J. J., "A Numerical Study of Thermal Effects on Flow and Pollutant Dispersion in Urban Street Canyons", J. Appl. Meteo., 38(9), pp. 1249-1261, (1998).

[20] Baik J. J. and Kim J. J., "A Numerical Study of Flow and Pollutant Dispersion Characteristics in Urban Street Canyons", J. Appl. Meteo., 38(11), pp. 1576-1589, (1999).

[21] Patankar S. V., "Numerical Heat Transfer and Fluid Flow", McGraw-Hill, New York, (1996).

[22] Ferziger J. H. and M. Perie, "Computational Methods for Fluid Dynamics", Springer Verlag Berlin Heidelberg, (1996).

[23] Costa M. J., Riethmuller M. L. and Borrego C., "Wind-tunnel simulation of gas dispersion over complex terrain: Comparison of two length-scale studies", Atmos. Environ., Vol. 28, No. 11, pp. 1933-1938, (1994).

[24] Robins A. G. and Castro I. P., "A Wind Tunnel investigation of plume dispersion in the vicinity of a surface mounted cube-I: the flow field", Atmos. Environ., Vol. 11, pp. 291-297, (1977).